Estimation of Vibrational Temperatures of N_2 and CO_2 in Low-Pressure Electron Cyclotron Resonance Plasmas by Threshold Ionization Mass Spectrometry

Shinnosuke HOSOYAMA, Masahiro YAMAZAKI and Koichi SASAKI

Division of Applied Quantum Science and Engineering, Hokkaido University, Sapporo 060-8628, Japan

(Received 16 March 2022 / Accepted 23 April 2022)

This paper demonstrates the estimation of vibrational temperatures of N_2 and CO_2 in low-pressure plasmas by threshold ionization mass spectrometry. The principle for the estimation is the decrease in the ionization potential by the vibrational excitation. We observed that the threshold ionization curves of N_2 and CO_2, which were measured using a quadrupole mass spectrometer with an energy-variable electron beam, shifted toward the low-energy side, when they were sampled from the plasmas. We constructed a model which assumed a Boltzmann distribution for the population densities of vibrational excited states and the same cross sections of electron impact ionization for vibrational excited states except the shifts of the threshold energies. The vibrational temperatures were estimated by fitting the experimental threshold ionization curves with the model.

Keywords: threshold ionization mass spectrometry, vibrational temperature, molecular nitrogen, carbon dioxide, low-pressure plasma

DOI: 10.1585/pfr.17.1406070

1. Introduction

Recently, vibrational excited states of molecular species attract much attention of many researchers in conjunction with gas conversion processes using plasmas. It is believed that vibrational excited states are useful for the improvement of the energy efficiency in CO_2 splitting [1–5]. This is because dissociation via an electronic excited state with a repulsive potential curve needs excess excitation energy between the dissociated state and the potential energy of the electronic excited state. CO_2 at the electronic ground state can be dissociated if it is excited to the vibrational state with $v_3 = 21$ [6], where v_3 is the vibrational quantum number for the asymmetric stretching mode of CO_2, and in this case we can avoid the useless consumption of the excess excitation energy in the Franck-Condon dissociation process.

The importance of vibrational excited states of molecular species is also pointed out in plasma-assisted catalytic reactions [7–9]. It is reported by Rettner and coworkers that vibrational excited states of molecular hydrogen have larger probabilities of dissociative adsorption than the vibrational ground state on Cu(111) [10]. In addition, more recent experiments using molecular beams show the enhancement of the reaction probabilities of CH_4 and CO_2 by the vibrational excitations [11, 12]. In general, vibrational temperatures of molecular species in nonequilibrium plasmas are higher than gas temperatures. Hence, many researchers expect that nonequilibrium plasmas are useful for enhancing the rates of catalytic reactions.

We need a method for measuring the vibrational temperatures of molecular species to investigate gas conversion processes in which vibrational excited states play important roles. However, the measurement of the vibrational temperature in a nonequilibrium plasma is an issue especially in a low-pressure plasma. Fourier-transform infrared spectroscopy (FTIR) [13, 14] and laser Raman scattering [14–16] are standard methods, but their signals are not detectable at a low pressure ($\leq$ 10 Pa). In addition, FTIR is a hard method for detecting vibrational excited states of CO_2, since we should exclude CO_2 from the optical passes among the light source, the Fourier-transform spectrometer, the detector, and the plasma. Optical emission spectroscopy is a simpler method and is applicable to a low-pressure plasma [17–19]. However, this method gives us the vibrational temperatures of electronic excited states, and the vibrational temperature of the electronic ground state, which is the majority even in a plasma, may be different from those of electronic excited states.

In this work, we developed a simple method for estimating vibrational temperatures of molecular species in nonequilibrium plasmas with low gas pressures. The method was based on threshold ionization mass spectrometry. Threshold ionization mass spectrometry is widely used for measuring densities of neutral radicals in the field of low-temperature reactive plasmas [20–23]. It utilizes the difference between the ionization potential of a radical and the potential for dissociative ionization of its parent molecule. Unlike this principle, the idea for measuring the vibrational temperature by threshold ionization mass spec-

author's e-mail: sasaki@qe.eng.hokudai.ac.jp

trometry is the decrease in the ionization potential by the vibrational excitation. We tried to derive the information of the vibrational population distribution from the threshold ionization curve.

2. Principles

Threshold ionization mass spectrometry needs a mass spectrometer with an energy-variable electron beam for ionizing neutral species sampled into it. In this work, we employed a commercial quadrupole mass spectrometer (QMS). If we sample molecules from a gaseous medium (but not a plasma), the QMS signal at a mass number (M/e) is given by

$$I_{\mathrm{g}}(E_{\mathrm{e}}) = \frac{\alpha J_{\mathrm{e}} n}{\sqrt{E_{\mathrm{e}}}} \int_0^{\infty} \sigma_0(\varepsilon)\, \sqrt{\varepsilon} f(\varepsilon) \mathrm{d}\varepsilon, \tag{1}$$

where E_{e} and J_{e} are the energy and the current density of the electron beam, respectively, n is the density of molecular species to be analyzed, $f(\varepsilon)$ is the energy distribution function of the electron beam, $\sigma_0(\varepsilon)$ is the cross section of electron impact ionization for the molecule at the vibrational ground state, and α is the proportional constant including the transport efficiency, the quantum yield in the secondary electron multiplier, *etc*. $I(E_{\mathrm{e}}) = \alpha J_{\mathrm{e}} n \sigma_0(E_{\mathrm{e}})$ if $f(\varepsilon)$ is approximated by the delta function. However, the broadening of the electron energy distribution function is not negligible, and in this work we assumed a Gaussian distribution for $f(\varepsilon)$ as follows,

$$f(\varepsilon) = \frac{1}{\Delta E_{\mathrm{e}}} \sqrt{\frac{\ln 2}{\pi}} \exp\left[-\ln 2 \left(\frac{\varepsilon - E_{\mathrm{e}}}{\Delta E_{\mathrm{e}}} \right) \right], \tag{2}$$

where ΔE_{e} denotes the half width at half maximum of the energy distribution function.

The population densities of vibrational excited states are not negligible when molecules are sampled from a plasma. In this case, electron impact ionization of vibrational excited states contributes to the QMS signal such that

$$I_{\mathrm{p}}(E_{\mathrm{e}}) = \frac{\alpha J_{\mathrm{e}}}{\sqrt{E_{\mathrm{e}}}} \sum_{v=0}^{\infty} n(v) \int_0^{\infty} \sigma_v(\varepsilon)\, \sqrt{\varepsilon} f(\varepsilon) \mathrm{d}\varepsilon, \tag{3}$$

where $n(v)$ is the population density of the vibrational state with the vibrational quantum number v, and $\sigma_v(\varepsilon)$ is the electron impact ionization cross section for the vibrational state. We assumed the Boltzmann distribution for $n(v)$,

$$n(v) = \frac{n}{U(T_{\mathrm{v}})} \exp\left(-\frac{E(v)}{kT_{\mathrm{v}}} \right), \tag{4}$$

with

$$U(T_{\mathrm{v}}) = \sum_{v=0}^{\infty} \exp\left(-\frac{E(v)}{kT_{\mathrm{v}}} \right), \tag{5}$$

where $E(v)$ is the energy of the vibrational state (the energy standard is $E(0)$), T_{v} is the vibrational temperature, and k is the Boltzmann constant.

The principle of the proposed method is the fitting between Eq. (3) and the corresponding threshold ionization curve observed experimentally. The problem here is the electron impact ionization cross section. The data for the vibrational ground state ($\sigma_0(\varepsilon)$) is known, but the cross section data for $v \geq 1$ are not available. In this work, we have employed a bold assumption that the cross sections of electron impact ionization are the same for the vibrational ground state and excited states except the shifts of the threshold energies. The magnitudes of the shifts were assumed to be equal to the vibrational energies. This is a reasonable assumption since the cross section of electron impact ionization is determined by the electronic transition and is basically independent of the state of the nuclei. Under this assumption, the QMS signal for a molecule sampled from a plasma is given by

$$I_{\mathrm{p}}(E_{\mathrm{e}}) = \frac{\alpha J_{\mathrm{e}}}{\sqrt{E_{\mathrm{e}}}} \sum_{v=0}^{\infty} n(v) \int_0^{\infty} \sigma_0(\varepsilon + E(v))\, \sqrt{\varepsilon} f(\varepsilon) \mathrm{d}\varepsilon. \tag{6}$$

3. Experiment

The experimental apparatus is schematically shown in Fig. 1. We used a miniature electron cyclotron resonance (ECR) plasma source, which employed permanent magnets for the ECR magnetic field, in this experiment. The diameter of the plasma source was 40 mm. It was connected to a microwave power supply at 2.45 GHz via a coaxial cable and a three-stab tuner. The microwave power was lower than 100 W. We tried the estimations of the vibrational temperatures of N_2 and CO_2 in pure N_2 and CO_2 plasmas, respectively. The plasma chamber was evacuated using a turbomolecular pump, and the operating pressures of N_2 and CO_2 were less than 1 Pa. The gas in the plasma was sampled into another chamber with differential pumping via an orifice with a diameter of 0.5 mm. The differentially pumped chamber was equipped with QMS (HIDEN Analytical HAL201). A collisionless condition was real-

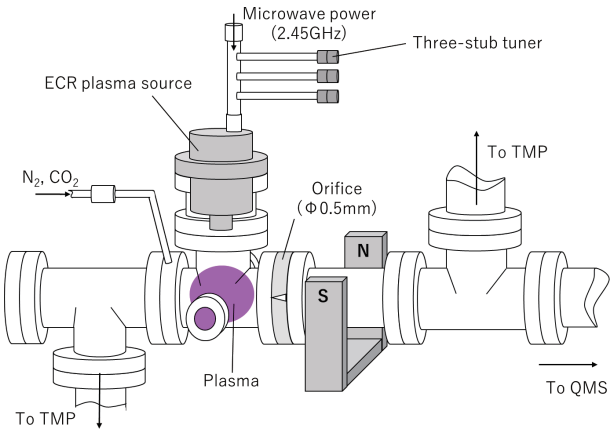

Fig. 1 Schematic of experimental apparatus.

ized in the QMS chamber since the pressure was lower than 5×10^{-6} Torr. We confirmed that the electron emission current was controlled to be independent of E_e in this QMS. The vacuum tube which connected the orifice and QMS was sandwiched by a pair of permanent magnets. The permanent magnets were necessary to reduce the noise in the QMS current which was caused by the direct transport of ions from the plasma.

4. Results

4.1 Estimation of electron energy distribution function

First of all, we examined the threshold ionization curves of Ar and N_2 to estimate the energy distribution function of the electron beam in QMS. Figure 2 (a) shows the threshold ionization curve of Ar together with the cross section of electron impact ionization. The cross section data was obtained from the LXCat database [24, 25]. Ar was introduced into the plasma chamber and a part of it was sampled into the QMS chamber via the orifice. The plasma was not ignited. As shown in the figure, the variation of the QMS signal agreed well with the cross section at $E_e \geq 18$ eV. However, the variation of the QMS signal was gentler than the cross section at electron energies around the ionization potential ($E_e \simeq 15.8$ eV). This discrepancy suggested the fact that the electron energy distribution function was not approximated by the delta function. The comparison between the threshold ionization curve and Eq. (1) is shown in Fig. 2 (b), where we assumed $0.2 \leq \Delta E_e \leq 0.6$ eV for the half width at half maximum of the electron energy distribution function. The signals are normalized at $E_e = 24$ eV. It was necessary to shift the calculated ionization curves by 0.5 eV toward the high-energy side to obtain the fitting shown in Fig. 2 (b), suggesting the inaccuracy in the absolute electron energy in QMS. As shown in the figure, we obtained the agreement between the experimental threshold ionization curve and Eq. (1) by assuming $\Delta E_e = 0.4$ eV. It was possible to evaluate the magnitude of the energy shift and the width of the electron energy distribution function independently.

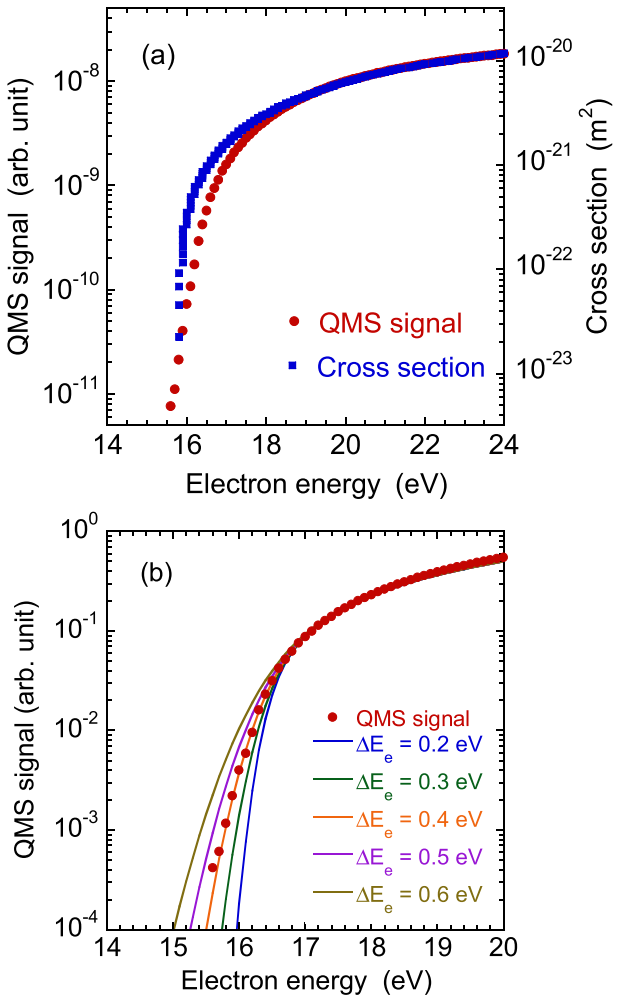

Fig. 2 (a) Comparison between threshold ionization curve of Ar and the cross section of electron impact ionization. (b) Comparison between threshold ionization curve of Ar and Eq. (1) with various values of ΔE_e.

We repeated the same comparison for N_2, as shown in Fig. 3. The cross section data was also obtained from the LXCat database [24]. As shown in Fig. 3 (a), the variation of the QMS signal was gentler than the cross section at electron energies around the ionization potential ($E_e \simeq 15.6$ eV). Figure 3 (b) shows the fitting between the experimental threshold ionization curve and Eq. (1). The signals are normalized at $E_e = 25$ eV. We shifted the calculated ionization curves by 0.95 eV toward the high-energy side to obtain the fitting shown in Fig. 3 (b). In the experiment, we observed the day-to-day fluctuation between 0.2 and 1 eV in the magnitude of the energy shift that was necessary to obtain the fitting, suggesting that the absolute electron energy in QMS was not stable. However, the day-to-day fluctuation was not a problem in the estimation of the vibrational temperature, since we checked the threshold ionization curve in every experiment. As shown in Fig. 3 (b), the threshold ionization curve observed experimentally was reproduced by Eq. (1) by assuming $\Delta E_e = 0.4$ eV. On the basis of the fitting results shown in Figs. 2 (b) and 3 (b), we concluded that the electron energy distribution function in QMS was represented by Eq. (2) with $\Delta E_e = 0.4$ eV.

4.2 Estimation of vibrational temperature of N_2

Figure 4 (a) shows the comparison between the threshold ionization curves of N_2 which were observed with and without the N_2 plasma. The N_2 pressure in the plasma chamber was 0.3 Pa, and the microwave power was 100 W. As shown in the figure, when the plasma was switched on, we observed a considerable current at the electron energy less than the ionization threshold of N_2. This was a kind of noise which was caused by the transport of N_2^+ from

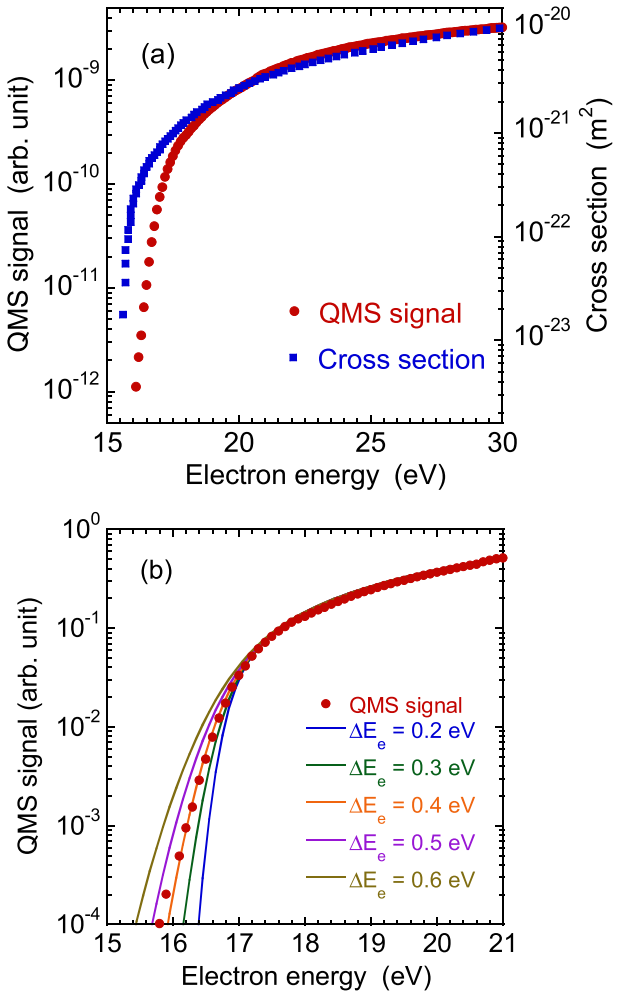

Fig. 3 (a) Comparison between threshold ionization curve of N_2 and the cross section of electron impact ionization. (b) Comparison between threshold ionization curve of N_2 and Eq. (1) with various values of ΔE_e.

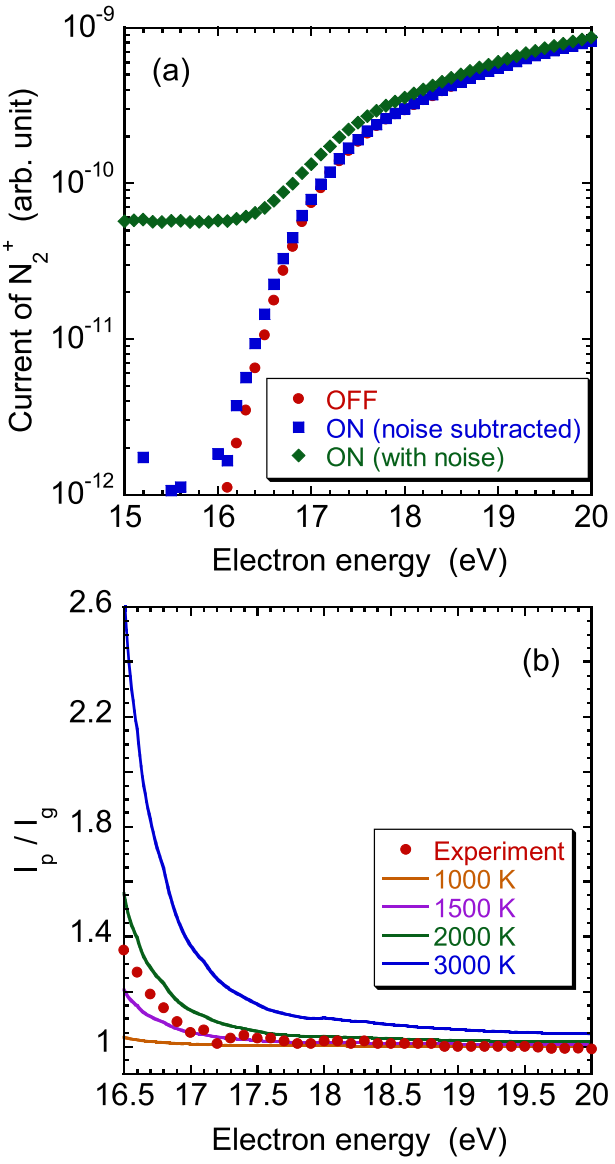

Fig. 4 Threshold ionization curves for estimating vibrational temperature of N_2. (a) Comparison between threshold ionization curves observed with and without plasma and (b) I_p/I_g at various T_v together with the ratio of blue and red plots shown in (a).

the plasma to the secondary electron multiplier in QMS. The noise was dependent on the plasma density and the plasma potential. We subtracted the noise from the current by fitting it with an exponential curve. The reason for employing the exponential curve was that we observed a straight line in the semilogarithmic plot for the noise, as shown in Fig. 4 (a). The QMS current after the subtraction of the noise shifted toward the low-energy side around the threshold energy, as shown in Fig. 4 (a), suggesting the contribution of vibrational excited states to the QMS signal.

We calculated the ratio I_p/I_g by adopting $\Delta E_e = 0.4$ eV. The vibrational energies $E(v)$ were calculated using the harmonic oscillator model with the vibrational constants of N_2 [26], and the population densities $n(v)$ were calculated at various T_v. We included vibrational excited states with $v \leq 5$ in the calculation, since the population densities for $v \geq 6$, which have energies higher than 1.83 eV, were negligible at a vibrational temperature less than 5000 K. The ratios I_p/I_g at various T_v are plotted in Fig. 4 (b) together with the experimental result (the ratio between the red and blue plots in Fig. 4 (a)). Considering the inaccuracy in the subtraction of the noise, the range for the comparison was limited at $E_e \geq 16.5$ eV. On the basis of the comparison shown in Fig. 4 (b), we estimated $T_v = 1800 \pm 100$ K for the vibrational temperature of N_2. The error bar was evaluated by the ambiguity in the comparison between I_p/I_g and the experimental result.

The vibrational temperature of N_2 thus estimated is summarized in Fig. 5. The increase in T_v with the microwave power was observed, as shown in Fig. 5 (a), where the N_2 pressure was fixed at 0.3 Pa. The increase in T_v is synchronized with the increase in the electron density, since vibrational excited states are produced by electron

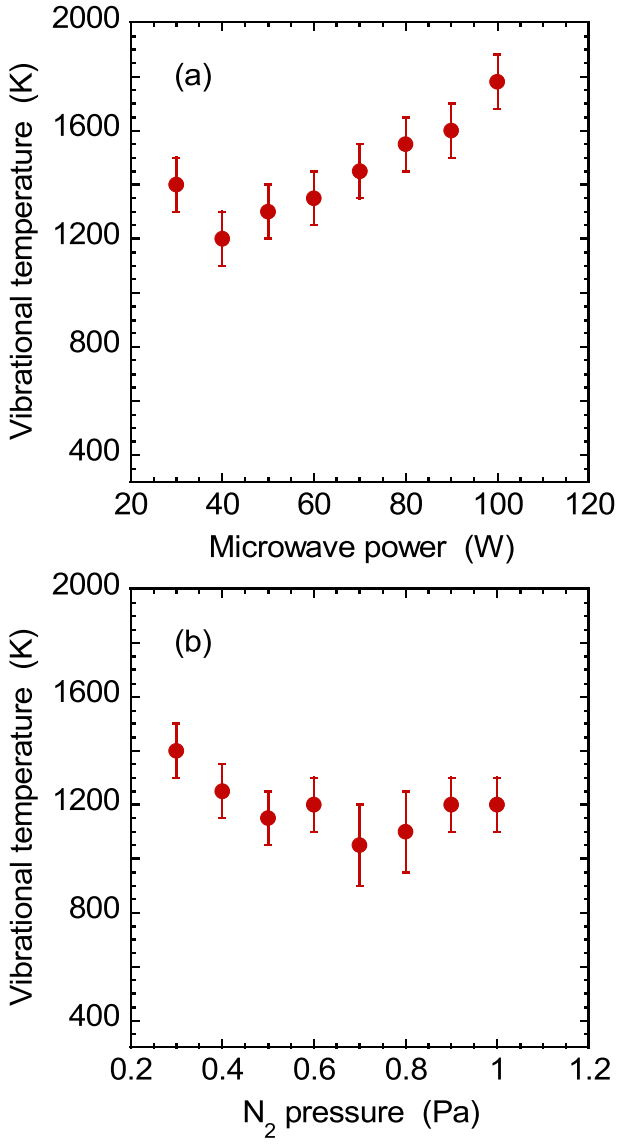

Fig. 5 Relationships between vibrational temperature of N_2 and discharge parameters. (a) T_v vs. microwave power and (b) T_v vs N_2 pressure.

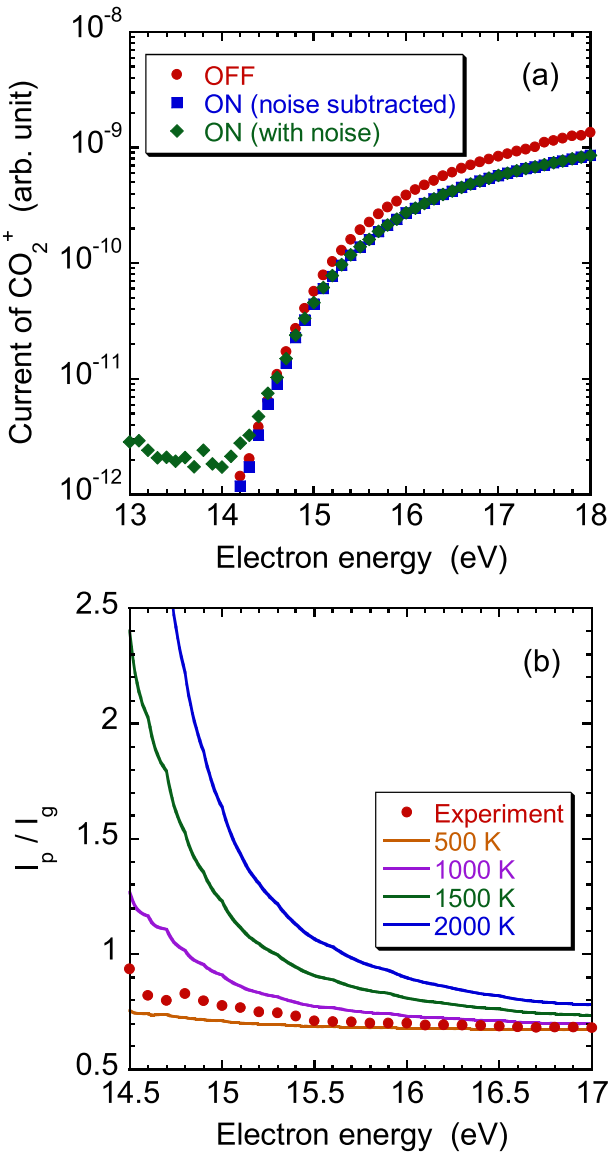

Fig. 6 Threshold ionization curves for estimating vibrational temperature of CO_2. (a) Comparison between threshold ionization curves observed with and without plasma and (b) I_p/I_g at various T_v together with the ratio of blue and red plots shown in (a).

impact excitation. On the other hand, we observed weak dependence of T_v on the pressure, as shown in Fig. 5 (b), where the microwave power was fixed at 30 W. The electron density increases with the pressure, but the increase in the rate of electron impact excitation may be compensated by the higher frequency of vibrational-translational energy transfer at the higher pressure, resulting in the weak dependence of T_v on the N_2 pressure.

4.3 Estimation of vibrational temperature of CO_2

We repeated a similar experiment and a calculation for CO_2. Since CO_2 has three vibrational modes, the number of vibrational excited states is much larger than that of N_2. The number of vibrational excited states we considered in the model for CO_2 was 520, even though we ignored the vibrational states with energies higher than 2 eV. The vibrational energies were calculated by

$$\frac{E_{CO_2}}{hc} = \sum_i \omega_i(v_i + d_i/2) + \sum_{j\geq i} \chi_{ij}(v_i + d_i/2)(v_j + d_j/2) + \chi_{l_2 l_2} l_2^2, \quad (7)$$

where h and c are the Plank constant and the speed of light, respectively, v_i and l_2 are the quantum numbers of the vibrational modes, and $d_1 = 1$, $d_2 = 2$, and $d_3 = 1$ are their degeneracies. The spectroscopic constants ω_i, χ_{ij}, and $\chi_{l_2 l_2}$ are shown in literature [6, 27].

Figure 6 (a) shows the threshold ionization curves of CO_2 observed with and without the plasma. The CO_2 pres-

sure and the microwave power were 1 Pa and 20 W, respectively. The noise caused by the transport of ions to QMS was smaller than that shown in Fig. 4 (a), which was due to the lower plasma density in the CO_2 plasma. In contrast to N_2, CO_2 had a high degree of dissociation, resulting in the decrease in the QMS current by the plasma production. The degree of dissociation estimated from Fig. 6 (a) was approximately 33%. The ratios I_p/I_g at various T_v are plotted in Fig. 6 (b) together with the experimental result. n in Eq. (4) was multiplied by 0.67 in calculating I_p to take the degree of dissociation into consideration. According to the comparison shown in Fig. 6 (b), we estimated $T_v = 700 \pm 100$ K for CO_2 in the plasma. The range for the comparison was limited at $E_e \geq 14.5$ eV, considering the inaccuracy in the subtraction of the noise caused by the transport of CO_2^+.

5. Discussion

The minimum vibrational temperatures that can be estimated using the proposed method are 1000 and 500 K for N_2 and CO_2, respectively, as understood from Figs. 4 (b) and 6 (b). On the other hand, the accuracy of the vibrational temperature estimated by the proposed method is affected by both the experiment and the model. The most serious problem in the present experiment was the noise due to the transport of ions from the plasma. The transport of ions to the orifice was unavoidable since the plasma potential was higher than the potential of the plasma chamber. We used a pair of permanent magnets to deflect ions in the tube that connected the orifice and QMS, but the fraction of ions arrived at QMS was considerable especially in the N_2 plasma, as shown in Fig. 4 (a). The ranges of the electron energy that were used for the comparison between the experimental ionization curves and I_p/I_g were limited at $E_e \geq 16.5$ eV and $E_e \geq 14.5$ eV in the N_2 and CO_2 plasmas, respectively, to avoid the error caused by the inaccuracy in the subtraction of the noise in the present experiment, but the detection limit and the ambiguity in the estimation of T_v may be improved if we can use the data at closer energies to the ionization potential. Mass spectrometers which have the ability of retarding ions are available commercially, and the use of such mass spectrometers may give us a better detection limit and improved ambiguity.

Another problem in the experimental point of view is the broadening of the electron energy distribution function. The width of $\Delta E_e = 0.4$ eV is rather narrow in comparison with the values in conventional quadrupole mass spectrometers, but a narrower broadening is preferable in the proposed method. We used the ranges of $16.5 \leq E_e \leq 18$ eV and $14.5 \leq E_e \leq 16.5$ eV for estimating the vibrational temperatures of N_2 and CO_2, respectively. Although ΔE_e is narrower than the ranges of the electron energy, the sharpness of I_p/I_g against E_e is damaged by the broadened electron energy distribution function. If we can use a spectrometer with narrower ΔE_e, we may obtain a better detection limit and improved ambiguity.

The principal problem in the model is the assumption of the Boltzmann distribution for the population densities of vibrational excited states. Vibrational population distributions which deviate from the Boltzmann distributions are observed experimentally [16, 28]. If the vibrational population distribution has a tail component, it may result in the over estimation of the vibrational temperature by the proposed method. In addition, different vibrational temperatures were observed for the different vibrational modes of CO_2 in plasmas (the vibrational temperature of the asymmetric stretching mode is higher than those of the symmetric stretching and bending modes) [13, 29, 30]. We have not ever observed a threshold ionization curve that is apparently deviated from the Boltzmann distribution in our experiment, but it is better to consider the possibility of the nonequilibrium population distribution in the data analysis.

6. Conclusions

We have demonstrated the estimation of the vibrational temperatures of N_2 and CO_2 on the basis of the threshold ionization curves which can be measured using a commercial quadrupole mass spectrometer. The principle of the estimation is the decrease in the ionization potential by the vibrational excitation. We observed the shifts of the threshold ionization curves toward the low-energy side, when the molecules were sampled from the plasmas. We compared the shifted threshold ionization curves with a model, and we estimated the vibrational temperatures. We believe that the proposed method is useful for estimating vibrational temperatures of molecular species in low-pressure plasmas.

Acknowledgments

This work was supported by JST CREST Grant Number JPMJCR19R3.

[1] P. Capezzuto, F. Cramarossa, R. d'Agostino and E. Molinari, J. Phys. Chem. **80**, 882 (1976).
[2] T. Nunnally, K. Gutsol, A. Rabinovich, A. Fridman, A. Gutsol and A. Kemoun, J. Phys. D: Appl. Phys. **44**, 274009 (2011).
[3] D.L. Pietanza, G. Colonna, G. D'Ammando, A. Laricchiuta and M. Capitelli, Plasma Sources Sci. Technol. **24**, 042002 (2015).
[4] C. Stewig, S. Scüttler, T. Urbanietz, M. Böke and A. von Keudell, J. Phys. D: Appl. Phys. **53**, 125205 (2020).
[5] M. Yamazaki, S. Nishiyama and K. Sasaki, Plasma Sources Sci. Technol. **29**, 115016 (2020).
[6] T. Kozak and A. Bogaerts, Plasma Sources Sci. Technol. **23**, 045004 (2014).
[7] Z. Sheng, Y. Watanabe, H.-H. Kim, S. Yao and T. Nozaki, Chem. Eng. J. **399**, 125751 (2020).
[8] Z. Sheng, H.-H. Kim, S. Yao and T. Nozaki, Phys. Chem. Chem. Phys. **22**, 19349 (2020).
[9] X. Chen, Z. Sheng, S. Murata, S. Zen, H.-H. Kim and T. Nozaki, J. CO2 Utilization **54**, 101771 (2021).

[10] C.T. Rettner, D.J. Auerbach and H.A. Michelsen, Phys. Rev. Lett. **68**, 1164 (1992).
[11] H. Ueta, L. Chen, R.D. Beck, I. Colon-Diaz and B. Jackson, Phys. Chem. Chem. Phys. **15**, 20526 (2013).
[12] J. Quan, F. Muttaqien, T. Kondo, T. Kozarashi, T. Mogi, T. Imabayashi, Y. Hamamoto, K. Inagaki, I. Hamada, Y. Morikawa and J. Nakamura, Nat. Chem. **11**, 722 (2019).
[13] B.L.M. Klarenaar, R. Engeln, D.C.M. van den Bekerom, M.C.M. van de Sanden, A.S. Morillo-Candas and O. Guaitella, Plasma Sources Sci. Technol. **26**,115008 (2017).
[14] E. Plönjes, P. Palm, W. Lee, M.D. Chidley, I.V. Adamovich, W.R. Lempert and J.W. Rich, Chem. Phys. **260**, 353 (2000).
[15] D.C.M. van den Bekerom, A. van de Steeg, M.C.M. van de Sanden and G.J. van Rooij, J. Phys. D: Appl. Phys. **53**, 054002 (2020).
[16] J. Kuhfeld, N.D. Lepikhin, D. Luggenhölscher and U. Czarnetzki, J. Phys. D: Appl. Phys. **54**, 305204 (2021).
[17] N. Britun, M. Gaillard, A. Ricard, Y.M. Kim, K.S. Kim and J.G. Han, J. Phys. D: Appl. Phys. **40**, 1022 (2007).
[18] T. Silva, N. Britun, T. Godfroid and R. Snyders, Plasma Sources Sci. Technol. **23**, 025009 (2014).
[19] T. Sakamoto, H. Matsuura and H. Akatsuka, J. Appl. Phys. **101**, 023307 (2007).
[20] H. Sugai and H. Toyoda, J. Vac. Sci. Technol. A **10**, 1193 (1992).
[21] S. Agarwal, G.W.W. Quax, M.C.M. van de Sanden, D. Maroudas and E.S. Aydila, J. Vac. Sci. Technol. A **22**, 71 (2004).
[22] J. Benedikt, S. Agarwal, D. Eijkman, W. Vandamme, M. Creatore and M.C.M. van de Sanden, J. Vac. Sci. Technol. A **23**, 1400 (2005).
[23] J. Osaka, M. Senthil Kumar, H. Toyoda, T. Ishijima, H. Sugai and T. Mizutani, Appl. Phys. Lett. **90**, 172114 (2007).
[24] Biagi database, www.lxcat.net, retrieved on December 23, 2021.
[25] L.C. Pitchford, L.L. Alves, K. Bartschat, S.F. Biagi, M.C. Bordage, A.V. Phelps, C.M. Ferreira, G.J.M. Hagelaar, W.L. Morgan, S. Pancheshnyi, V. Puech, A. Stauffer and O. Zatsarinny, J. Phys. D: Appl. Phys. **46**, 334001 (2013).
[26] NIST Chemistry webbook, https://webbook.nist.gov/chemistry/
[27] I. Suzuki, J. Mol. Spectrosc. **25**, 479 (1968).
[28] W. Lee, I.V. Adamovich and W.R. Lempert, J. Chem. Phys. **114**, 1178 (2001).
[29] Y. Du, T.V. Tsankov, D. Luggenhölscher and U. Czarnetzki, J. Phys. D: Appl. Phys. **54**, 34LT02 (2021).
[30] Y. Du, T.V. Tsankov, D. Luggenhölscher and U. Czarnetzki, J. Phys. D: Appl. Phys. **54**, 365201 (2021).